

# ROUGH SURFACE PLASTICITY AND ADHESION ACROSS LENGTH SCALES

Yan-Fei Gao and Allan F. Bower

*Division of Engineering, Brown University, Providence, RI 02912, USA, Tel: +1-401-863-2864; Fax: +1-401-863-9009; Email: Yanfei\_Gao@brown.edu*

**Abstract:** The study of interacting rough surfaces, especially at mesoscale and nanoscale, has been playing a central role in a broad spectrum of novel applications, e.g. nanostructure fabrication and reliability. The multiscale nature of surface roughness, the structure- and size-sensitive material deformation behavior, and the importance of surface forces and other physical interactions give rise to very complex surface phenomena at mesoscale and nanoscale. In this work, we present a contact mechanics model based on the power spectral density function of the surface roughness. This is more relevant to large-scale rough surface contact with the use of classic plasticity theory. If using phenomenological strain-gradient plasticity theory, we can show that one can only flatten asperities in a certain frequency interval of the roughness spectrum. We also present a new scheme of modeling rough surface adhesion by using the Dugdale model and the self-affine fractal surface, which leads to a discussion of gecko adhesion. We also present some of our perspectives about the interaction between adhesion and micro-plasticity for, e.g., nano-imprinting and nano-welding applications.

**Key words:** Multiscale roughness, roughness evolution, size-dependent plasticity, rough surface adhesion, micromechanics of surface plasticity.

## 1. INTRODUCTION

Solid-solid interactions of rough surfaces, especially at mesoscale and nanoscale, govern many important mechanical and physical properties for a number of novel applications, including nanostructure fabrication and reliability (e.g. nano-imprinting, nano-welding, chemical mechanical planarization, MEMS stiction), soft material adhesion, nanostructured

coating design, friction and wear, among many others [1-2]. The classic work of rough surface contact is the Greenwood-Williamson (GW) model [3], which models the surface roughness as a collection of uniform asperities with a Gaussian height variation and gives a statistical way to deduce multi-asperity contact from single-asperity contact. Certainly this model has its advantages in the study of many engineering surfaces, but not appropriate for the small scale rough surface mechanics for the following three reasons.

(1) Surface roughness typically has a multiscale nature, i.e. the existence of roughness details at many length scales [4-5]. Statistical parameters defined in the GW model depend on the measurement window size and instrument resolution, so that cannot describe surface roughness uniquely. It should also be noted that the fractal description is only one example of multiscale roughness.

(2) Deformation mechanisms at small scale are very complicated. There have been a lot of experimental evidences that plastic deformation is size-dependent [6]. In addition, rough surfaces could also be sources and sinks of dislocations, leading to so-called surface plasticity. We can use phenomenological strain-gradient plasticity theories based on Taylor hardening rule at microscale [6-7], or study the cooperative behaviors of defects and the interaction with rough surfaces at nanoscale [8-9].

(3) Surface forces and adhesion play an important role for small scale structural integrity [10], for example, in MEMS stiction problem. It's more interesting to study the coupling behavior between adhesion and surface plasticity. Physical forces from less familiar origins (e.g. surface stress) may also be pronounced when the feature size is reduced.

The above three aspects and their interactions contribute to the complex surface phenomena at mesoscale and nanoscale. The theme objective of this paper is to examine scaling relations and scale effects for multiscale modeling of rough surface plasticity and adhesion. Future emphasis will be placed on how to link atomic and mesoscale contacts.

## 2. LARGE-SCALE ROUGH SURFACE CONTACT

The GW model describes a rough surface by the rms height  $\sigma$ , rms slope  $\sigma'$  and rms curvature  $\sigma''$  [3,11-12]. Unfortunately, because of the fractal nature of surface roughness, those statistical parameters depend on the measurement window size and instrument resolution. As a consequence, we shall characterize the surface roughness by the power spectral density function (PSDF), which is the Fourier transform of the autocorrelation function [4-5,11]. Figure 1 shows a typical rough surface topography and the corresponding PSDF. For an ideally self-affine fractal surface, the PSDF is a

straight line with respect to  $\omega$ , and the slope tells the fractal dimension. In reality, there is a low-frequency cutoff due to component size, surface inhomogeneity or grain size. The high-frequency cutoff is usually due to the measurement resolution, though the ideal fractal roughness is not expected to extend to nanoscale. It should be noted that our following contact analysis is not restricted to fractal description of surface roughness.

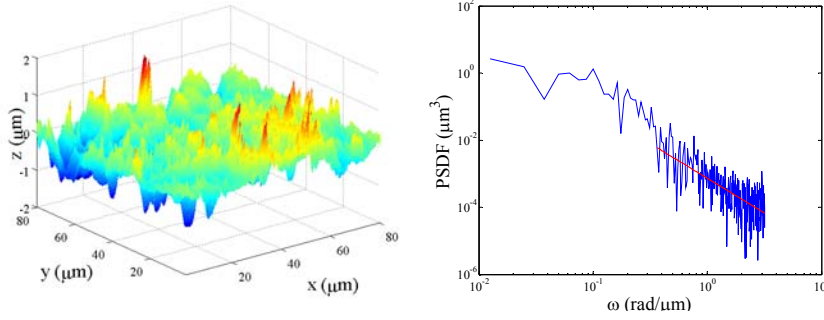


Figure 1. (a) AFM topography of single crystal Cu. (b) Fractal properties can be deduced from the power spectral density function, using the line information at  $y \sim 20 \mu\text{m}$  in (a). The straight line is by least squares fitting, giving rise to fractal dimension  $D \sim 1.5$ .

The self-affine fractal rough surface can be idealized by using a Weierstrass function of the form

$$z(x) = A_0 \sum_{n=0}^{\infty} \gamma^{(D-2)n} \cos(2\pi\gamma^n x / \lambda_0) \quad (1)$$

where  $A_0$  and  $\lambda_0$  are amplitude and wavelength of the zero-th scale, and  $\gamma$ ,  $D$  ( $1 < D < 2$ ) are scale-independent, dimensionless parameters that characterize the fractal properties. We can approximate the PSDF of Eqn. 1 by a continuous one, which is proportional to  $\omega^{2D-5}$  [4].

Rough surface contact analyses can be categorized into three types. (1) The GW model is based on the height distribution of isolated asperities. Although it gives a neat statistical means of deducing multi-asperity contact from single-asperity contact, the roughness description is not appropriate, as discussed in previous section. We have to introduce an artificial cutoff high-frequency in order to obtain meaningful statistical parameters for the GW model. (2) Direct numerical simulations are usually difficult to cover the whole spectrum of asperities, because asperity feature sizes range over many length scales and much smaller than the component size. Some hybrid schemes inherit drawbacks of GW-type statistical models. The calculation is usually limited by the cutoff size of mesh and asperity measurement

resolution. While refining the mesh size and measurement resolution, we would observe endless contact details. However, a microstructurally relevant length-scale might give a meaningful cutoff if we are concerned with certain failure analysis. (3) Many fractal-based contact models [4,13], out of thin air, give the contact size distribution directly from the “bearing-area” relation, and sum up all possible isolated asperity contacts. Actually, the true contact size distribution by our following contact analysis is radically different.

The contact mechanics based on self-affine fractal roughness, however, remains a challenge [14-17]. We recently establish an elastic-plastic contact analysis based on Archard’s method and Weierstrass series [17]. Refer to Fig. 1 again. Idealizing a self-affine fractal rough surface by the Weierstrass function, we bridge two successive scales in the roughness spectrum by the assumption that the nominal pressure at the fine scale is equal to the true pressure at the coarse scale. Of course, this is justified if asperities at successive scales have large difference in contact compliance (usually true if successive wavelengths are far apart). If two successive scales are quite close, clearly we cannot decouple the roughness scales, and the contribution to the contact compliance from the fine scales must be included.

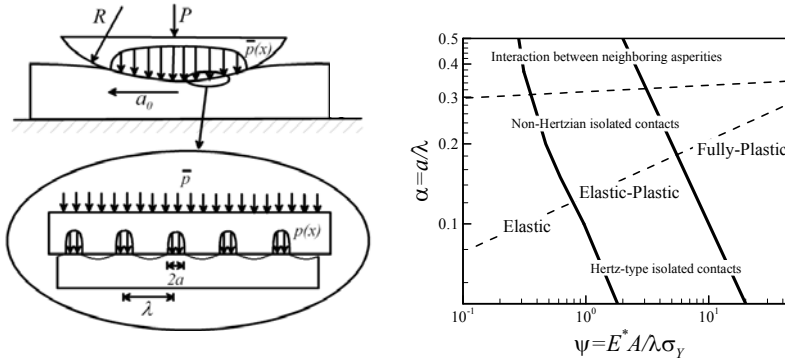


Figure 2. (a) Schematic of rough surface contact in Archard’s manner. (b) Indentation map illustrating the deformation characteristics of sinusoidal surface.

As shown by the schematic in Fig. 2(a), we can compute the contact properties of the scale  $n$  from the scale  $n - 1$ . Fig. 2(b) gives the indentation map of sinusoidal contact, which can be characterized by two parameters:  $\alpha = a/\lambda$  and  $\psi = E^* A/\lambda \sigma_y$ , where  $a$  is the contact half-width,  $A$  is the amplitude and  $\lambda$  is the period of the sinusoidal surface,  $E^*$  is the effective modulus and  $\sigma_y$  is the yield stress of the elastic-perfectly plastic solid. Most importantly, when  $2a \rightarrow \lambda$ , we have significant interaction between neighboring asperities. For a sufficiently large  $\psi$ , as the contact fraction increases, the contact pressure first reaches the material hardness  $H \sim 3\sigma_y$ ,

and then rises up to a value  $H^* \sim 6\sigma_Y$ . It should also be noted that this transitional behavior is weakly dependent on the asperity shape as long as it is wedge-like.

For elastic multiscale contact, the analysis is rather complicated. *Assuming the asperity pressure distribution be uniform*, we can easily derive the scaling relations for the contact fraction and the contact pressure when the roughness scale is sufficiently large. The asymptotic solution for the contact fraction is  $2\alpha_{n \rightarrow \infty} = \gamma^{1-D}$ , and the total contact area is

$$L_n / \lambda_0 \approx 0.4 \gamma^{-(D-1)(n-1)} \tilde{p} \quad (2)$$

with  $\tilde{p} = F / \pi E^* A_0$ . The contact is supported by infinite number of zero-size contact spots, each of which has infinite contact pressure. Such an understanding is also evident by the FEM calculation. If we refine mesh size and include more asperities at smaller scales, the pressure distribution will evolve from rather smooth to quite spike-like [17-18]. Of course, fine scale contact cannot be elastic. Plasticity or others may change this conclusion.

The critical wavelength of plastic-yield can be easily computed, using  $2\alpha_{n \rightarrow \infty} = \gamma^{1-D}$ . The calculation gives  $\lambda_{cr} \approx \lambda_0 \psi_0^{1/(D-1)}$ . The plastic deformation therefore is confined to a thin layer near the surface, with the width comparable to  $\lambda_{cr}$ . The above result is only valid when  $\psi_0$  is small. Our latest work [17] gives a complete analysis.

Now consider rigid-plastic contact of self-affine fractal surface (i.e., very large  $\psi$ ). If the contact pressure is limited by material hardness, with a given load  $F$ , the total contact area is  $L_n \equiv F/H$ . Because of the pressure rise-up feature in Fig. 2(b), and the fact that nominal pressure at fine scale is limited by true pressure at coarse scale, the fine-scale contact can never reach complete contact, namely, asperity persistence at every roughness scale. The contact area as  $n \rightarrow \infty$  is  $L_{n \rightarrow \infty} = F/H^*$ .

An important conclusion from the above analysis is that a perfectly fractal description of surface roughness ( $1 < D < 2$ ) appears to lead to unphysical predictions of the true contact size and number of contact spots, for both elastic and elastic-plastic solids. It is anticipated that either non-fractal roughness (but possibly multiscale), or micro-plasticity, or adhesion might resolve this open question.

### 3. ROUGHNESS EVOLUTION AND MICROMECHANICS OF SURFACE PLASTICITY

Experimentally, we can measure the change of PSDF before and after contact loading, a potential link between contact analysis of surface failure

mechanisms. Load-displacement curves, e.g. [19], wouldn't contain enough information about surface deformation. Because of self-affine fractal roughness, smaller asperities are rougher and large frequencies deform mainly plastically. The critical wavelength of elastic-plastic transition approximately happens at  $\lambda_0 \psi_0^{1/(D-1)}$ , also drawn schematically in Fig. 3(a).

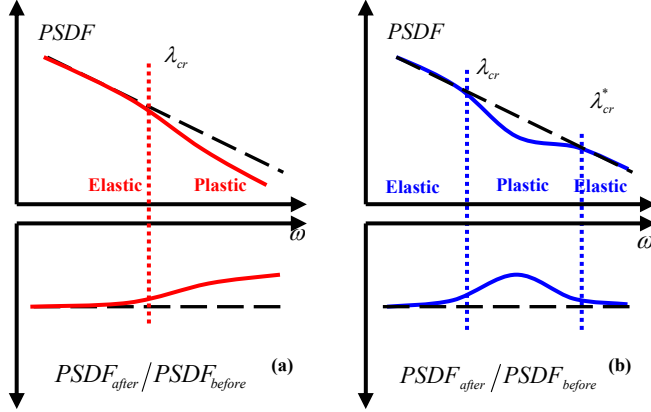


Figure 3. Schematics of the evolution of power spectral density function.

We also conjecture that at very high frequency, plastic deformation is difficult to realize because of small size. Thus there would be another critical scale beyond which asperities deform elastically, and only an intermediate range of frequencies can be plastically crushed and likely smoothed. This can be proved by using the phenomenological strain-gradient plasticity theory by Nix and Gao [6], which is a statistical description of dislocation interaction based on Taylor hardening rule. The material hardness  $H$  is given by  $H/H_0 = \sqrt{1 + \hat{l}\chi}$ , where  $H_0$  can be explained as bulk hardness,  $\hat{l}$  is a material length scale, and  $\chi$  is the strain gradient. Approximately  $\chi \sim$  asperity slope/contact size. The Weierstrass surface roughness in Eqn. 1 tells us that asperity slope increases rapidly with respect to roughness scale  $n$ . Our calculations shows that the plastic-elastic transition occurs at the critical wavelength  $\lambda_{cr}^* \approx \lambda_0 (A_0/\hat{l})^{1/(1-B/2)}$ , as shown in Fig. 3(b).

However, we should be very careful about this result, because the Nix-Gao theory is based on bulk defects. The size effects of nanoindentation also depend on surface roughness. Even though roughness is confined into a very thin layer, the resulted plastic deformation can extend to a very far depth. We need to clarify the contribution to the size effects from bulk contact and surface roughness. The usefulness of strain gradient plasticity may be very limited. It's more reasonable to carry out a micromechanics analysis of defects. We need to consider the plastic deformation due to the novel surface property and surface geometry, and the interaction with surface and bulk

defect structures. This can be denoted as micromechanics of surface plasticity.

The work in [9] considers the indentation of a stepped surface. The surface ledge can be regarded as an existing pileup dislocation. Dislocations can emit from this ledge and may or may not pile up underneath. Because of adhesion and long-range dislocation interaction, we also need to model the lateral interaction between neighboring ledges. It is anticipated that dislocation mechanics study can bridge the scale gap between AFM-based nanotribology and mesoscale phenomena such as nano-imprinting.

#### 4. EFFECTS OF ROUGHNESS ON ADHESION

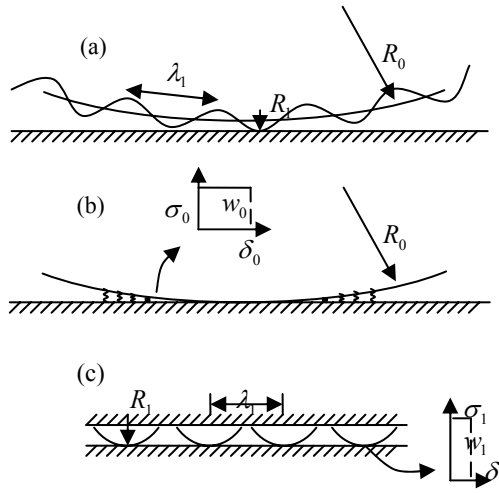


Figure 4. (a) A two-scale adhesive contact with superposition of spheres. Cohesive zone properties in coarse-scale contact in (b) are deduced from fine-scale contact in (c).

When studying the effect of roughness on adhesion, we need to proceed from the finest scale, in contrast to the top-down manner in the rough surface contact analysis. Consider the schematic in Fig. 5, in which the two-scale rough surface obeys Eqn. 1. Assume asperity contact at scale 1 is JKR-like [10,20-22], i.e.  $\delta_1 \rightarrow 0$  while  $w_1$  remains finite. For isolated, spherical asperity contact, the pull-off force is  $F_c \sim w_1 R_1$  with corresponding separation  $\delta_c \sim (w_1^2 R_1 / E^{*2})^{1/3}$ . The equivalent cohesive zone in Figure 5(b), with strength  $\sigma_0$  and characteristic bridging-length  $\delta_0$ , has the following properties:  $\sigma_0 \sim F_c / \lambda_1^2$  and  $\delta_0 \sim \delta_c$ , where  $1/\lambda_1^2$  is the asperity density at scale 1. Consequently, the apparent work of adhesion at scale 0 is

$$w_0 = \sigma_0 \delta_0 \sim \frac{w_1 R_1}{\lambda_1^2} \left( \frac{w_1^2 R_1}{E^{*2}} \right)^{1/3} \sim w_1 \left( \frac{w_1 \lambda_1}{E^* A_1^2} \right)^{2/3}, \text{ or } \frac{w_0}{w_1} \sim \frac{1}{\alpha_1^2} \quad (4)$$

where  $\alpha_1 = (E^* A_1^2 / w_1 \lambda_1)^{1/3}$  determines whether the contact at fine scale 1 is adhesive or elastic. Thus the apparent work of adhesion at coarse scale depends on the contact characteristics of the fine scale. If fine scale contact is adhesive,  $\alpha_1 \ll 1$ , then  $w_0/w_1 > 1$ . If fine scale contact is elastic,  $\alpha_1 \gg 1$ , then  $w_0/w_1 < 1$ .

The above simple analysis [23] shows the importance of morphology on adhesion. It should be noted that the adhesion strength depends on the apparent work of adhesion as well as the contact area, which is determined by the contact analysis from the long wavelength. Thus, whether a rough surface is “adhesive” depends on the morphology and the loading history.

In addition, adhesive contact of isolated asperity is not appropriate for a self-affine fractal rough surface. For non-isolated contact, consider a sinusoidal surface with amplitude  $A$  and period  $\lambda$ . Define two dimensionless parameters  $\alpha = (E^* A^2 / w \lambda)^{1/3}$  and  $\beta = \sigma_0 (\lambda^2 / w E^{*2} A)^{1/3}$ . Small  $\alpha$  gives rise to adhesive contact, and large  $\alpha$  elastic contact. Small  $\beta$  gives rise to large scale bridging (LSB), and *cohesive zone may spread to the whole period*. Large  $\beta$  gives small scale bridging (SSB). With varying  $\alpha$  and  $\beta$ , we can have a variety of contact behaviors. We may have a critical roughness scale beyond which the roughness does not contribute to the adhesion.

By the GW model, roughness only attenuates the adhesion. With the consideration of self-affine fractal roughness and non-isolated adhesive contact, we can get the opposite conclusion under certain conditions. Strong adhesion can be attained by obtaining a large true contact area (since roughness can also increase the contact compliance), and keeping the large-scale-bridging feature (to increase the fracture strength), at every roughness scale. For gecko adhesion, those are attained by the hierarchical structure of gecko foot, which can also accommodate a wide range of roughness frequencies. From the computational point of view, we can simulate the adhesion of rough surfaces by using either cohesive zone model [24] or molecular simulation [25-26], and interpret the results as in Fig. 5.

## 5. COUPLING OF ADHESION AND PLASTICITY

For MEMS stiction and many new nanofabrication methods [27], the strong adhesion between rough surfaces is critically affected by the surface plasticity. The plastic deformation during asperity separation can

dramatically increase the apparent work of adhesion. A fundamental understanding of coupling adhesion and surface plasticity is eagerly needed.

Johnson's approximate analysis [10] shows that small contact size and low hardness promotes the ductile separation, which therefore is often observed in nanoscale molecular simulations and large-scale contact of extremely soft metal (indium, for example). However, the contact behavior at mesoscale is still poorly understood. Though plastic deformation can increase the work of adhesion, surface roughness can do the opposite. Also the size-dependent surface plasticity is less studied along this line.

Rough surface plasticity and adhesion at the mesoscale would be the link between atomic and macroscopic contacts. It is anticipated that mesoscale adhesive contact could be promoted or weakened, depending on the coupling between adhesion and micromechanics of surface plasticity. Therefore, we have a large degree of freedom to either bond, imprint and/or peel two rough surfaces at nano- and meso-scale.

## 6. SUMMARY

In this work, we first present a contact mechanics model based on the power spectral density function of the surface roughness, and give the elastic-plastic contact analysis. Size-dependent plasticity shows that one can only flatten asperities in a certain frequency interval of the roughness spectrum. But the most important topic is micro-mechanics of surface plasticity, which studies the dislocation nucleation and interaction with the rough surface. We also present a new scheme of modeling rough surface adhesion by using the Dugdale model and self-affine fractal surface, which leads to a morphology- and history-dependent cohesive zone law.

## ACKNOWLEDGEMENTS

This work is supported by the Brown/General Motors Collaborative Research Lab at Brown University. We are very grateful to discussions with Prof. K.-S. Kim (Brown) and Drs. Y.-T. Cheng, L. Lev and Y. Qi (GM).

## REFERENCES

1. Singer IL, Pollock HM. *Fundamentals of friction: macroscopic and microscopic processes*, Kluwer Academic, Boston, 1992.
2. Bhushan B. *Handbook of micro/nanotribology*, CRC Press, 1999.

3. Greenwood JA, Williamson JBP. "Contact of nominally flat surfaces", *Proc. R. Soc. Lond. A*, **vol. 295**, pp. 300-319, 1966.
4. Majumdar A, Bhushan B. "Fractal model of elastic-plastic contact between rough surfaces", *ASME J. Tribol.*, **vol. 113**, pp. 1-11, 1991.
5. Greenwood JA, Wu JJ. "Surface roughness and contact: an apology", *Meccanica*, **vol. 36**, pp. 617-630, 2001.
6. Nix WD, Gao H. "Indentation size effects in crystalline materials: a law for strain gradient plasticity", *J. Mech. Phys. Solids*, **vol. 46**, pp. 411-425, 1998.
7. Bhushan B, Nosonovsky M. "Scale effects in friction using strain gradient plasticity and dislocation-assisted sliding (microslip)", *Acta Mater.*, **vol. 51**, pp. 4331-4345, 2003.
8. Hurtado JA, Kim K-S. "Scale effects in friction of single-asperity contacts. I. From concurrent slip to single-dislocation-assisted slip", *Proc. R. Soc. Lond. A*, **vol. 455**, pp. 3363-3384, 1999. "II. Multiple-dislocation-cooperated slip", *ibid*, pp. 3385-3400.
9. Yu HH, Shrotriya P, Wang J, Kim K-S. 2004, "Dislocation nucleation and segregation in nano-scale contact of stepped surfaces", *Mat. Res. Soc. Symp. Proc.*, **vol. 795**, 7.9, 2004.
10. Johnson KL. "Mechanics of adhesion", *Tribol. Int.*, **vol. 31**, pp. 413-418, 1998.
11. Greenwood JA. "A unified theory of surface roughness", *Proc. Roy. Soc. Lond. A*, **vol. 393**, pp. 133-157, 1984.
12. McCool JJ. "Comparison of models for the contact of rough surface", *Wear*, **vol. 107**, pp. 37-60, 1986.
13. Yan W, Komvopoulos K. "Contact analysis of elastic-plastic fractal surfaces", *J. Appl. Phys.*, **vol. 84**, pp. 3617-3624, 1998.
14. Archard JF. "Elastic deformation and the laws of friction", *Proc. R. Soc. Lond. A*, **vol. 243**, pp. 190-205, 1957.
15. Ciavarella M, Demelio G, Barber JR, Jang YH. "Linear elastic contact of the Weierstrass profile", *Proc. R. Soc. Lond. A*, **vol. 456**, pp. 387-405, 2000.
16. Persson BNJ. "Elastoplastic contact between randomly rough surfaces", *Phys. Rev. Lett.*, **vol. 87**, art no. 116101, 2001.
17. Gao YF, Bower AF. Submitted for publication, 2004.
18. Borri-Brunetto M, Carpinteri A, Chiaia B. "Scaling phenomena due to fractal contact in concrete and rock fractures", *Int. J. Fract.*, **vol. 95**, pp. 221-238, 1999.
19. Buzio R, Boragno C, Biscarini F, de Mongeot FB, Valbusa U. "The contact mechanics of fractal surfaces", *Nature Mater.*, **vol. 2**, pp. 233-236, 2003.
20. Johnson KL, Kendall K, Roberts AD. "Surface energy and the contact of elastic solids", *Proc. R. Soc. Lond. A*, **vol. 324**, pp. 301-313, 1971.
21. Derjaguin BV, Muller VM, Toporov YP. "Effect of contact deformations on the adhesion of particles", *J. Coll. Interface Sci.*, **vol. 53**, pp. 314-326, 1975.
22. Maugis D. "Adhesion of spheres: the JKR-DMT transition using a Dugdale model", *J. Coll. Interface Sci.*, **vol. 150**, pp. 243-269, 1992.
23. Gao YF, Bower AF. Unpublished work, 2004.
24. Gao YF, Bower AF. "A simple technique for avoiding convergence problems in finite element simulations of crack nucleation and growth on cohesive interfaces", *Modelling Simul. Mater. Sci. Eng.*, **vol. 12**, pp. 453-463, 2004.
25. Qi Y, Cheng Y-T, Cagin T, Goddard III WA. "Friction anisotropy at Ni(100)/(100) interfaces: molecular dynamics studies", *Phys. Rev. B*, **vol. 66**, art no. 085420, 2002.
26. Cha P-R, Srolovitz DJ, Vanderlick TK. "Molecular dynamics simulation of single asperity contact", *Acta Mater.*, **vol. 52**, pp. 3983-3996, 2004.
27. Forrest SR. "The path to ubiquitous and low-cost organic electronic appliances on plastic", *Nature*, **vol. 428**, pp. 911-918, 2004.